

1 **Supplementary Information** for “*Winter Wonderland Cave, Utah, USA: A Natural Laboratory*
2 *for the Study of Cryogenic Cave Carbonate and Thawing Permafrost*”

3 **Jeffrey Munroe^{1*}, Kristin Kimble¹, Christoph Spötl², Gabriela Serrato Marks³, David**
4 **McGee³, and David Herron⁴**

5 ¹Geology Department, Middlebury College, Middlebury, VT 05753, USA.

6 ²Institute of Geology, University of Innsbruck, Innsbruck 6020, Austria.

7 ³Department of Earth, Atmospheric, and Planetary Sciences, Massachusetts Institute of
8 Technology, Cambridge, MA, 02142, USA.

9 ⁴USDA-Forest Service, Ashley National Forest, Duchesne, UT, 84021, USA.

10 *Corresponding author: Jeffrey Munroe (jmunroe@middlebury.edu)

11

12 **Sample Preparation and Analysis**

13 Individual CCC samples were separated into 3 size fractions to examine whether properties of
14 the CCCs differed with size. For each sample, wet sediment was scooped out of its plastic vial
15 with a clean spatula and deposited on a 250- μm mesh sieve over a clean beaker. Distilled water
16 and prodding from a spatula separated the sample components that were $>250\text{ }\mu\text{m}$, leaving the
17 $<250\text{-}\mu\text{m}$ fraction and water in the beaker. This solution was then poured through a 75- μm mesh
18 sieve over a second clean beaker and more distilled water separated the samples into 250-75- μm
19 and $<75\text{ }\mu\text{m}$ fractions. Each fraction was placed in a 50-mL centrifuge tube, and after fine
20 sediment had settled, excess water was carefully decanted. Samples were then frozen in a -40°C
21 freezer for 4 hours. The uncapped centrifuge tubes were then placed in a Labconco FreeZone 6
22 Liter freeze dryer and allowed to dry overnight. The resulting powder was ground with a clean
23 mortar and pestle and returned to each tube.

24

25 **Scanning Electron Microscopy**

26 A Tescan Vega 3 LMU scanning electron microscope (SEM) at Middlebury College was used to
27 acquire images of the CCC. All samples in different grain size fractions were adhered to metal
28 disks with double sided tape in preparation for analysis. Each metal disk was coated in gold
29 palladium, and images were captured for the three grain size fractions for each sample at
30 different magnifications in order to compare CCC morphologies. Energy dispersive x-ray
31 spectroscopy (EDS) was applied to samples YS-3, YS-6, TS-2, CP, YP, and TF after carbon
32 coating to determine if different grain morphologies observed under the SEM correspond to
33 different elemental compositions. The semi-quantitative elemental results were converted to
34 weight % oxides to differentiate between calcite, dolomite, and quartz. AZtecOne software was
35 used to capture secondary electron and backscatter images and for elemental analysis. Weight %
36 oxide data were transformed into structural formulae for common minerals.

37

38 **Grain Size Distribution**

39 The smallest size fraction (<75 μm) of each sample was analyzed using the HORIBA LA-950 to
40 determine its grain size distribution. Samples of the <75- μm fraction were centrifuged for 2
41 minutes and the liquid was poured off to yield a volume of \sim 25 mL. Then samples were
42 deflocculated for 30 seconds using a Vortex-T Genie 2, then sonified with an FS20D sonifying
43 water bath for 1 minute. A clean syringe was used to transfer liquid and sediment of each
44 sample into the HORIBA. Sample runs were duplicated to assess drift of the instrument over the
45 course of the analysis. The HORIBA grain size distribution data were presented as volume
46 percentages of sand (coarse, medium, and fine), silt (coarse, medium, fine, and very fine), clay
47 ($2\text{-}1 \mu\text{m}$), and colloid (<1 μm).

48

49 **X-ray Diffraction**

50 In preparation for bulk sample x-ray diffraction (XRD) analysis, dried samples were ground
51 using a ceramic mortar and pestle. Samples of the 250-75- μ m size fraction, as well as rock
52 samples powdered in a shatterbox, were analyzed on a Bruker D8 Advance Model X-Ray
53 Diffractometer at Middlebury College. The mineralogy of several samples was compared across
54 different size fractions (<75 μ m and 250-75 μ m) to detect any compositional differences. As no
55 obvious differences were detected, the grain size fractions <75 μ m and 250-75 μ m were used
56 interchangeably for future analyses depending on the volume of sample remaining. Nine
57 samples of the two size fractions were analyzed using the Random Powder Long Routine
58 (RPLR), which scans samples at 2-50° 2 Θ . Samples CP, YP, and TF did not have enough
59 material to fill a holder in the XRD, so they were transferred to a glass slide and analyzed using
60 an Oriented Powder Long Routine, which scans samples at 2-40° 2 Θ . The diffractometer
61 operated at 40 kV and 40 mA with a solid state detector, theta-theta goniometer, and CuK α
62 radiation. Mineral abundances were quantified using intensity ratios, and known mineral spectra
63 peaks were identified by comparison with standard reference patterns.

64

65 **X-ray Fluorescence**

66 CCC samples were analyzed for major element composition using x-ray fluorescence (XRF) at
67 Middlebury College. All samples were of the 75-250- μ m size fraction. Samples were heated in
68 a LECO TGA-701 thermogravimetric analyzer prior to XRF analysis to remove organics and
69 interstitial water. Dried samples were thoroughly ground into a fine powder and combined in a

70 10:1 ratio of lithium borate fluxing agent to sample (0.6000 g of sample and 6.000 g fluxing
71 agent). The combined sample and fluxing agent were melted in a Claisse LeNeo fluxer at 1050°
72 C for 22 minutes to form a glass disk. This process was repeated for five of the collected CCC
73 samples (YS-4, YS-6, TS-1, TS-2, and one rock sample); the other samples did not contain
74 sufficient mass in the desired particle size range for fluxing. Glass disks were analyzed using a
75 Thermo Scientific ARL QuantX energy dispersive (ED) XRF spectrometer to measure major
76 elements. A glass disk made from standard 88B (dolomitic limestone) was included in each run
77 to assess the quality of measurements. The analysis quantified the abundance of oxides, which
78 were converted to atomic abundances of major elements (Si, Ti, Al, Fe, Mn, Mg, Ca, Na, K, P).

79

80 **Inductively Coupled Plasma Mass Spectrometry**

81 Seven samples of the size fraction <75 µm (YS-3, YS-4, YS-5, YS-6, TS-1, TS-2, and a bedrock
82 sample), and an additional YS-4 sample of grain size 250-250 µm were prepared for analysis
83 with inductively coupled plasma mass spectrometry (ICP-MS) to determine the abundance of
84 trace and rare earth elements. Dried samples were combined in a 9:1 ratio of lithium metaborate
85 fluxing agent to sample (0.2000 g sample and 1.8000 g LiBO₂). A Claisse LeNeo fluxer was
86 used to melt the sample and fluxing agent and combine the melt with 5% HNO₃. Dissolution
87 was aided by a spinning magnetic bar. Dissolved samples were then transferred to a 100-mL
88 volumetric flask and HNO₃ was added to make 100 mL. This solution (T1) was transferred to a
89 125-mL polypropylene bottle as a 100× dilution of the original sample. An additional dilution
90 was made for trace element analysis by pipetting 5 mL of the T1 solution and 2 mL of an internal
91 standard solution containing 1 ppm Rh, In, Re, and Bi. Nitric acid was also added to this
92 solution to make 100 mL. This resulting T2 volume dilution was 2000×.

93 A Thermo Scientific iCAP Q ICP-MS was used in conjunction with Qtegra ISDS
94 software to analyze the dissolved CCC and rock samples, along with samples of water from the
95 cave. For each run, calibration curves were generated based on standard solutions specific to the
96 regular or trace elements method. Quality control with internal standards to drift correct was
97 conducted after every five samples. USGS rock standard 88B (dolomitic limestone) was
98 analyzed at the beginning and end of every batch of CCC samples, and standard 1643f was run in
99 conjunction with water samples. Data were synthesized with Qtegra software.

100

101 **C and O Stable Isotopes**

102 Eleven samples (all <75- μ m size fraction except CP and YP 250-75 μ m) were prepared for $\delta^{18}\text{O}$
103 and $\delta^{13}\text{C}$ stable isotope analysis in the Department of Geology at Union College. Roughly 0.09
104 mg of sample was weighed into glass vials and analyzed using a Thermo GasBench II connected
105 to a Thermo Delta Advantage mass spectrometer in continuous flow mode. Analytical
106 uncertainties were better than 0.1 ‰ (1σ) for $\delta^{18}\text{O}$ and 0.05 ‰ (1σ) for $\delta^{13}\text{C}$. All values were
107 calibrated against international standards and reported in permil (‰) relative to Vienna Pee Dee
108 belemnite (VPDB).

109 Eleven samples of bedrock, along with separate size fractions of samples YS-1 through
110 YS-6, CP, and YP were analyzed in the Institute for Geology at the University of Innsbruck.
111 Measurements were made on a Thermo Scientific Delta V Plus isotope ratio mass spectrometer
112 (IRMS) connected to a GasBench II¹. This system produces a typical precision (1σ) of $\pm 0.06\text{ ‰}$
113 for $\delta^{13}\text{C}$ and $\pm 0.08\text{ ‰}$ for $\delta^{18}\text{O}$ ². All samples were run in duplicate.

114

115 **$^{230}\text{Th}/^{234}\text{U}$ Disequilibrium Dating**

116 Five samples (YS-5, YS-6, CP, YP, and TF) were analyzed using U-Th radiometric dating
117 techniques in the Department of Earth, Atmospheric, and Planetary Sciences at the
118 Massachusetts Institute of Technology. Two samples were divided into three replicates (YS-5 A,
119 B, C and YS-6 A, B, C) to assess reliability of the dating for young samples with a high potential
120 for Th contamination. One replicate for each sample did not produce a result due to a low yield
121 in chemistry. Approximately 0.03 g of each sample was combined with a ^{229}Th - ^{233}U - ^{236}U tracer,
122 then digested and purified via iron coprecipitation and ion exchange chromatography. U and Th
123 were analyzed on separate aliquots using a Nu Plasma II-ES multi-collector ICP-MS equipped
124 with a CETAC Aridus II desolvating nebulizer following previously published protocols³. U-Th
125 ages were calculated using standard decay constants for ^{230}Th , ^{234}U , and ^{238}U ⁴⁻⁶. Ages were
126 recalculated under the assumption that the TF sample is modern, giving the sample a relative age
127 of -61 years BP (where present is defined as AD 1950). Reported errors for ^{238}U and ^{232}Th
128 concentrations are estimated to be $\pm 1\%$ due to uncertainties in spike concentration, while
129 analytical errors are smaller. Variability of initial $^{230}\text{Th}/^{232}\text{Th}$ throughout the cave is assumed to
130 be $\pm 25\%$ at 2σ .

131

132 **References Cited:**

133 1. Spötl, C. & Vennemann, T. W. Continuous-flow isotope ratio mass spectrometric analysis of
134 carbonate minerals. *Rapid communications in mass spectrometry* **17**, 1004–1006 (2003).

135 2. Spötl, C. Long-term performance of the Gasbench isotope ratio mass spectrometry system for
136 the stable isotope analysis of carbonate microsamples. *Rapid Communications in Mass*
137 *Spectrometry* **25**, 1683–1685 (2011).

138 3. Burns, S. J. *et al.* Rapid human-induced landscape transformation in Madagascar at the end of
139 the first millennium of the Common Era. *Quaternary Science Reviews* **134**, 92–99 (2016).

140 4. Jaffey, A. H., Flynn, K. F., Glendenin, L. E., Bentley, W. t & Essling, A. M. Precision
141 measurement of half-lives and specific activities of U 235 and U 238. *Physical review C* **4**,
142 1889 (1971).

143 5. Edwards, R. L., Gallup, C. D. & Cheng, H. Uranium-series dating of marine and lacustrine
144 carbonates. *Reviews in Mineralogy and Geochemistry* **52**, 363–405 (2003).

145 6. Cheng, H. *et al.* Improvements in 230 Th dating, 230 Th and 234 U half-life values, and U–Th
146 isotopic measurements by multi-collector inductively coupled plasma mass spectrometry.
147 *Earth and Planetary Science Letters* **371**, 82–91 (2013).

148

Table S1. CCC Samples Collected from Winter Wonderland Cave

Sample Name	Image	Location	Size Fractions	CCC type and mineralogy
YS-1		On ice surface	250-165 µm, 165-75 µm, <75 µm	CCC _{coarse} Calcite
YS-2		On ice surface	250-165 µm, 165-75 µm, <75 µm	CCC _{coarse} Calcite
YS-3		On ledge above ice surface	250-165 µm, 165-75 µm, <75 µm	CCC _{fine} Calcite, Quartz
YS-4		On ledge above ice surface	250-165 µm, 165-75 µm, <75 µm	CCC _{fine} Calcite, Quartz
YS-5		In moat at base of wall	250-165 µm, 165-75 µm, <75 µm	CCC _{coarse} Calcite

YS-6		From ice surface	250-165 µm, 165-75 µm, <75 µm	CCC _{coarse} Calcite
CP		From clear pool of water on ice surface	250-165 µm, 165-75 µm, <75 µm	CCC _{coarse} Calcite
YP		From yellow pool of water on ice surface	250-165 µm, 165-75 µm, <75 µm	CCC _{coarse} Calcite
TF		From surface of water amidst polygonal crystals	No size fractions, limited sample	CCC _{coarse} Calcite
BR		Collected <i>in situ</i> from near top of ice exposure	No size fractions, limited sample	CCC _{coarse} Calcite

150

151

Table S2. Isotope Results from Winter Wonderland Cave

Sample	Size fraction	Lab	$\delta^{18}\text{O}$	$\delta^{13}\text{C}$	Note
YS-1	Bulk	Union	-18.00	2.87	$\text{CCC}_{\text{coarse}}$
YS-2	Bulk	Union	-16.38	2.00	$\text{CCC}_{\text{coarse}}$
YS-3	Bulk	Union	-7.55	4.68	CCC_{fine}
YS-4	Bulk	Union	-7.09	7.28	CCC_{fine}
YS-5	Bulk	Union	-14.75	1.61	$\text{CCC}_{\text{coarse}}$
YS-6	Bulk	Union	-20.25	4.27	$\text{CCC}_{\text{coarse}}$
CP	Bulk	Union	-16.57	5.90	$\text{CCC}_{\text{coarse}}$
YP	Bulk	Union	-16.16	2.27	$\text{CCC}_{\text{coarse}}$
TF-1	Bulk	Union	-12.12	4.92	$\text{CCC}_{\text{coarse}}$
TF-2	Bulk	Union	-12.83	4.84	$\text{CCC}_{\text{coarse}}$
BF - 1a	Bulk	Innsbruck	-14.71	2.33	$\text{CCC}_{\text{coarse}}$
BF - 1b	Bulk	Innsbruck	-15.06	2.16	$\text{CCC}_{\text{coarse}}$
YS - 1 - 2a	165_250	Innsbruck	-12.86	6.03	More $\text{CCC}_{\text{coarse}}$ in finer fractions
YS - 1 - 2b	165_250	Innsbruck	-13.03	6.20	
YS - 1 - 3a	75_165	Innsbruck	-14.90	4.67	
YS - 1 - 3b	75_165	Innsbruck	-14.89	4.61	
YS - 1 - 4a	<75	Innsbruck	-17.72	2.79	
YS - 1 - 4b	<75	Innsbruck	-17.63	2.80	
YS - 2 - 2a	165_250	Innsbruck	-9.20	3.65	More $\text{CCC}_{\text{coarse}}$ in finer fractions
YS - 2 - 2b	165_250	Innsbruck	-9.39	3.59	
YS - 2 - 3a	75_165	Innsbruck	-14.43	3.05	
YS - 2 - 3b	75_165	Innsbruck	-14.52	3.05	
YS - 2 - 4a	<75	Innsbruck	-16.18	1.66	
YS - 2 - 4b	<75	Innsbruck	-16.25	1.62	
YS - 3	>250	Innsbruck	-9.48	6.76	CCC_{fine}
YS - 3 - 2a	165_250	Innsbruck	-14.75	2.17	
YS - 3 - 2b	165_250	Innsbruck	-14.60	2.15	
YS - 3 - 3a	75_165	Innsbruck	-8.83	2.69	
YS - 3 - 3b	75_165	Innsbruck	--	--	
YS - 3 - 4a	<75	Innsbruck	-7.46	4.30	
YS - 3 - 4b	<75	Innsbruck	-7.27	4.45	
YS - 4	>250	Innsbruck	-5.05	5.95	CCC_{fine}
YS - 4 - 2a	165_250	Innsbruck	-7.78	5.27	
YS - 4 - 2b	165_250	Innsbruck	-7.84	5.30	
YS - 4 - 3a	75_165	Innsbruck	-8.12	5.34	
YS - 4 - 3b	75_165	Innsbruck	-8.27	5.1	

YS - 4 - 4a	<75	Innsbruck	-7.21	6.96	
YS - 4 - 4b	<75	Innsbruck	-7.17	6.95	
YS - 5 - 2a	165_250	Innsbruck	-15.61	2.01	all CCC _{coarse}
YS - 5 - 2b	165_250	Innsbruck	-15.59	2.06	
YS - 5 - 3a	75_165	Innsbruck	-14.57	1.82	
YS - 5 - 3b	75_165	Innsbruck	-14.53	1.80	
YS - 5 - 4a	<75	Innsbruck	-14.37	1.33	
YS - 5 - 4b	<75	Innsbruck	-14.22	1.34	
CP - 2a	165_250	Innsbruck	-16.05	5.51	all CCC _{coarse}
CP - 2b	165_250	Innsbruck	-16.20	5.59	
CP - 3a	75_165	Innsbruck	-15.99	5.21	
CP - 3b	75_165	Innsbruck	-16.01	5.28	
CP - 4a	<75	Innsbruck	-15.52	4.77	
CP - 4b	<75	Innsbruck	-15.66	4.72	
YP - 2a	165_250	Innsbruck	-15.90	1.62	all CCC _{coarse}
YP - 2b	165_250	Innsbruck	-15.65	1.62	
YP - 3a	75_165	Innsbruck	-16.09	1.91	
YP - 3b	75_165	Innsbruck	-16.17	1.79	
YP - 4a	<75	Innsbruck	-16.11	1.46	
YP - 4b	<75	Innsbruck	-16.32	1.34	
BF - 1a	Bulk	Innsbruck	-14.71	2.33	
BF - 1b	Bulk	Innsbruck	-15.06	2.16	
TF - 1a	Bulk	Innsbruck	-12.54	4.82	
TF - 1b	Bulk	Innsbruck	-12.54	4.82	
YS - 6 - 2a	165_250	Innsbruck	-18.60	4.31	all CCC _{coarse}
YS - 6 - 2b	165_250	Innsbruck	-19.02	4.35	
YS - 6 - 3a	75_165	Innsbruck	-19.28	4.22	
YS - 6 - 3b	75_165	Innsbruck	-19.35	4.39	
YS - 6 - 4a	<75	Innsbruck	-18.29	4.12	
YS - 6 - 4b	<75	Innsbruck	-18.39	4.14	
WW - 1a	Rock	Innsbruck	-5.34	2.64	
WW - 1b	Rock	Innsbruck	-5.19	2.73	
SR-1	Rock	Innsbruck	-4.45	3.26	
SR-2	Rock	Innsbruck	-4.09	3.28	
SR-3	Rock	Innsbruck	-4.34	3.24	
CoD-1	Rock	Innsbruck	-13.37	-3.26	
CoD-2	Rock	Innsbruck	-8.20	0.66	Dolomite
CoD-3	Rock	Innsbruck	-3.55	3.04	Dolomite
FF-1	Rock	Innsbruck	-5.83	2.35	
FF-3-1	Rock	Innsbruck	-4.45	3.06	
By-6	Rock	Innsbruck	-4.04	4.08	
Alcove	Rock	Innsbruck	-6.21	2.29	

Table S3. Major Element Abundance in Samples from Winter Wonderland Cave*

Sample	Na ₂ O	MgO	Al ₂ O ₃	SiO ₂	P ₂ O ₅	K ₂ O	CaO	TiO ₂	MnO	Fe ₂ O ₃	Total
Bedrock	0.47	2.12	1.07	4.83	-0.09	0.08	89.42	0.06	0.02	0.52	98.51
YS-4 75-250 µm	0.05	1.84	4.88	52.19	0.11	1.11	39.12	0.22	0.14	1.76	101.41
YS-6 75-250 µm	0.45	12.16	2.03	9.55	0.85	0.86	70.70	0.07	0.02	0.56	97.25

154

*Presented as weight percent oxide

155

Table S4. Chondrite-Normalized REE Abundances for Samples from Winter Wonderland Cave

Sample	La	Ce	Nd	Sm	Eu	Gd	Dy	Er	Yb	Lu
YS-3 75 µm	69.9	67.4	28.4	15.6	6.9	10.4	9.0	9.0	10.1	10.3
YS-4 75 µm	50.6	49.8	20.8	11.6	5.5	7.8	6.4	6.3	6.9	6.7
YS-5 75 µm	12.6	8.4	4.4	1.9	0.6	1.1	0.9	1.0	1.1	1.0
YS-6 75 µm	13.4	9.1	4.6	1.9	0.5	1.0	0.7	0.9	1.0	1.1
WW rock	5.6	3.4	2.9	1.8	1.0	1.6	1.4	1.3	1.2	1.0
YS-4 75-250 µm	34.7	35.8	14.4	8.2	3.9	5.6	4.6	4.4	4.8	4.7

156

157

Table S5. U-Th Dating Results for CCC Samples from Winter Wonderland Cave

Sample ID	^{238}U (ng/g) ^a	$\pm (2\sigma)$	^{232}Th (pg/g) ^a	$\pm (2\sigma)$	$\delta^{234}\text{U}$ (per mil) ^b	$\pm (2\sigma)$	$^{230}\text{Th}/^{238}\text{U}$	$\pm (2\sigma)$	$^{230}\text{Th}/^{232}\text{Th}$ activity ppm atomic	$\pm (2\sigma)$	Age (yr) (uncorrected) ^c	$\pm (2\sigma)$	Age (yr) (corrected) ^d	$\pm (2\sigma)$	$\delta^{234}\text{U}$ initial (per mil) ^e	$\pm (2\sigma)$	Age (yr BP) (corrected) ^f	$\pm (2\sigma)$
KK-5A	577	12	346497	6930	995	2.9	0.4	0.012	9.3	0.3	20780	752	5829	4129	1012	12.2	5760	4129
KK-5C	592	12	412255	8247	959	1.7	0.4	0.014	9.2	0.3	24643	924	6780	5019	977	14.0	6711	5019
KK-6A	435	9	467240	9349	407	2.0	0.5	0.021	8.0	0.3	51244	2497	8622	13716	418	16.4	8553	13716
KK-6B	448	9	470609	9414	443	1.9	0.5	0.021	7.9	0.3	47886	2312	7681	12766	453	16.6	7612	12766
KK-CP	760	15	263625	5281	1309	1.3	0.2	0.007	8.2	0.3	8744	341	1451	1929	1314	7.3	1382	1929
KK-YP	530	11	249332	4994	1516	1.7	0.3	0.009	9.0	0.3	12114	439	3016	2434	1529	10.7	2947	2434
KK-TF	164	3	42729	856	836	2.1	0.1	0.005	6.9	0.3	6889	309	8	1811	836	4.8	-61	1811

Notes:

Samples KK-5A and KK6C had a low yield in chemistry and could not be dated

^aReported errors for ^{238}U and ^{232}Th concentrations are estimated to be $\pm 1\%$ due to uncertainties in spike concentration; analytical uncertainties are smaller.

^b $d^{234}\text{U} = (I^{234}\text{U}/I^{238}\text{U})_{\text{activity}} - 1 \times 1000$.

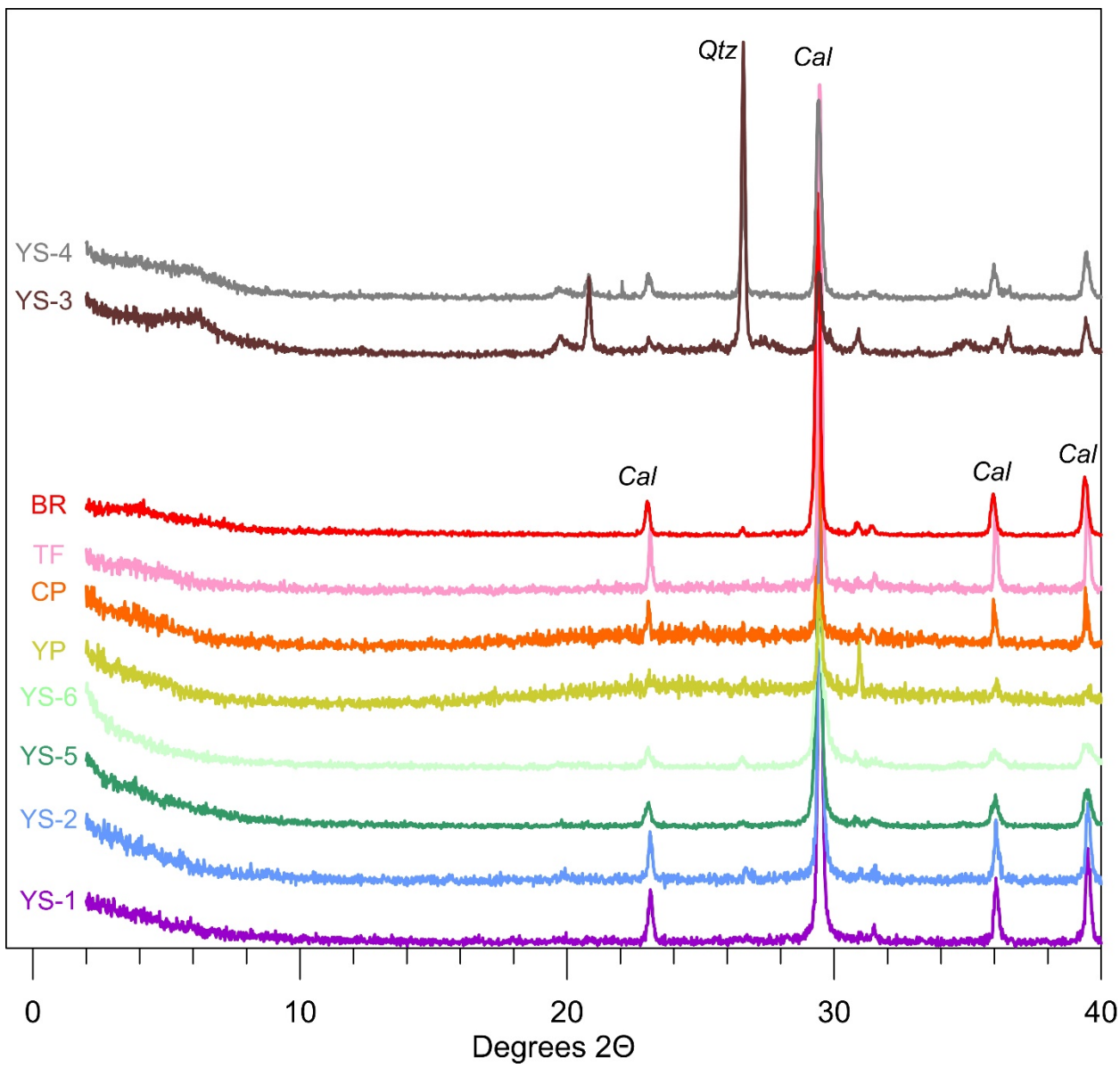
^c $I^{230}\text{Th}/I^{232}\text{Th}_{\text{activity}} = 1 - e^{-I^{230}\text{Th}T} + (d^{234}\text{U}_{\text{measured}}/10000) [I^{230}/(I^{230} - I^{232})] (1 - e^{-(I^{230} - I^{232})T})$, where T is the age. "Uncorrected" indicates that no correction has been made for initial ^{230}Th .

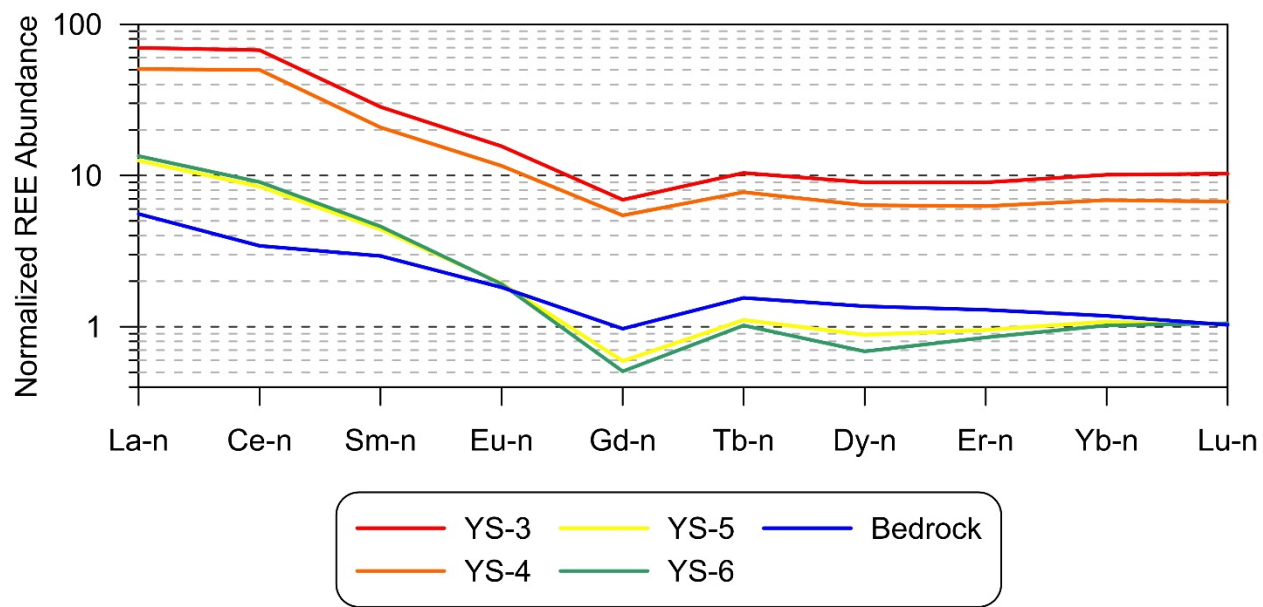
^dAges are corrected for detrital ^{230}Th assuming an initial $^{230}\text{Th}/^{232}\text{Th}$ of $(6.89 \pm 1.72) \times 10^{-6}$, based on the $^{230}\text{Th}/^{232}\text{Th}$ of sample KK-TF and an assumed $\pm 25\%$ 2-sigma uncertainty.

^e $d^{234}\text{U}_{\text{initial}}$ corrected was calculated based on ^{230}Th age (T), i.e., $d^{234}\text{U}_{\text{initial}} = d^{234}\text{U}_{\text{measured}} \times e^{I^{234}T}$, and T is corrected age.

^fB.P. stands for "Before Present" where the "Present" is defined as the January 1, 1950 C.E.

Decay constants for ^{230}Th and ^{234}U are from Cheng et al. (2013); decay constant for ^{238}U is $1.55125 \times 10^{-10} \text{ yr}^{-1}$ (Jaffey et al., 1971).

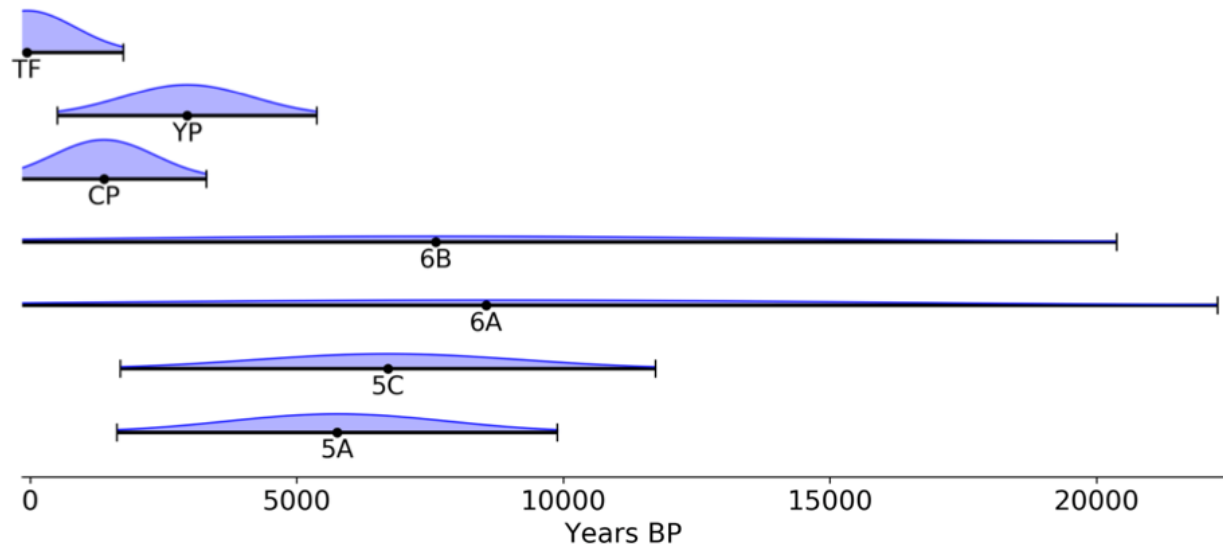




166
167

168 **Figure S2:** Rare earth element (REE) patterns for samples from Winter Wonderland Cave,
169 normalized to a chondrite standard. REEs are notably more abundant in the two CCC_{fine} samples
170 (YS-3 and YS-4), consistent with a greater detrital component.

171
172

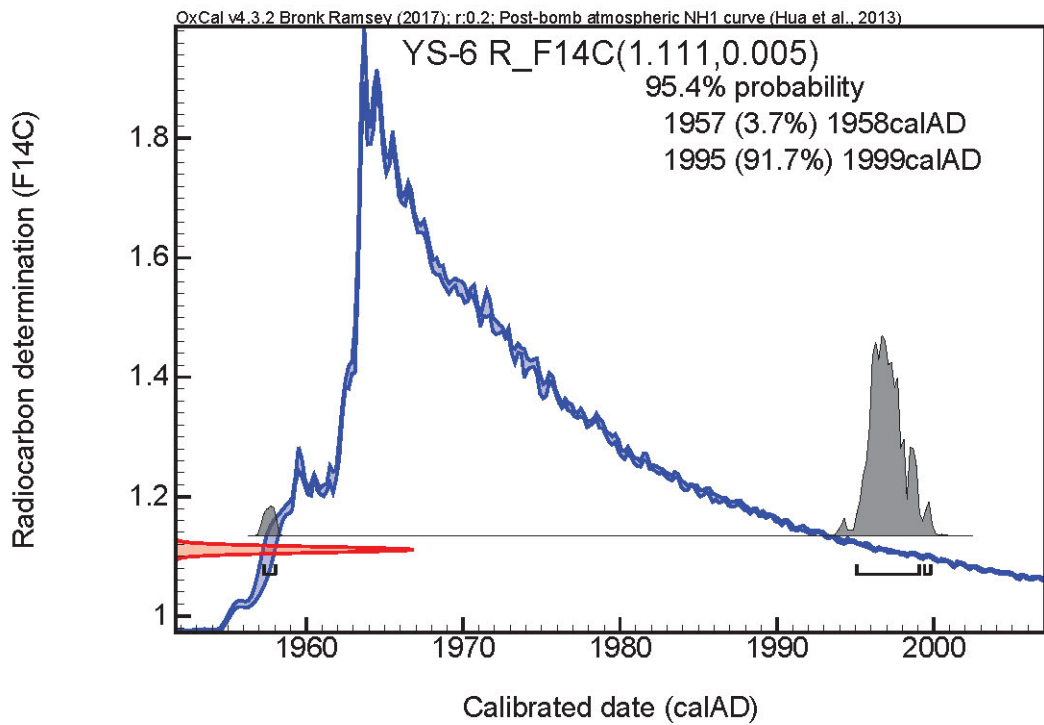


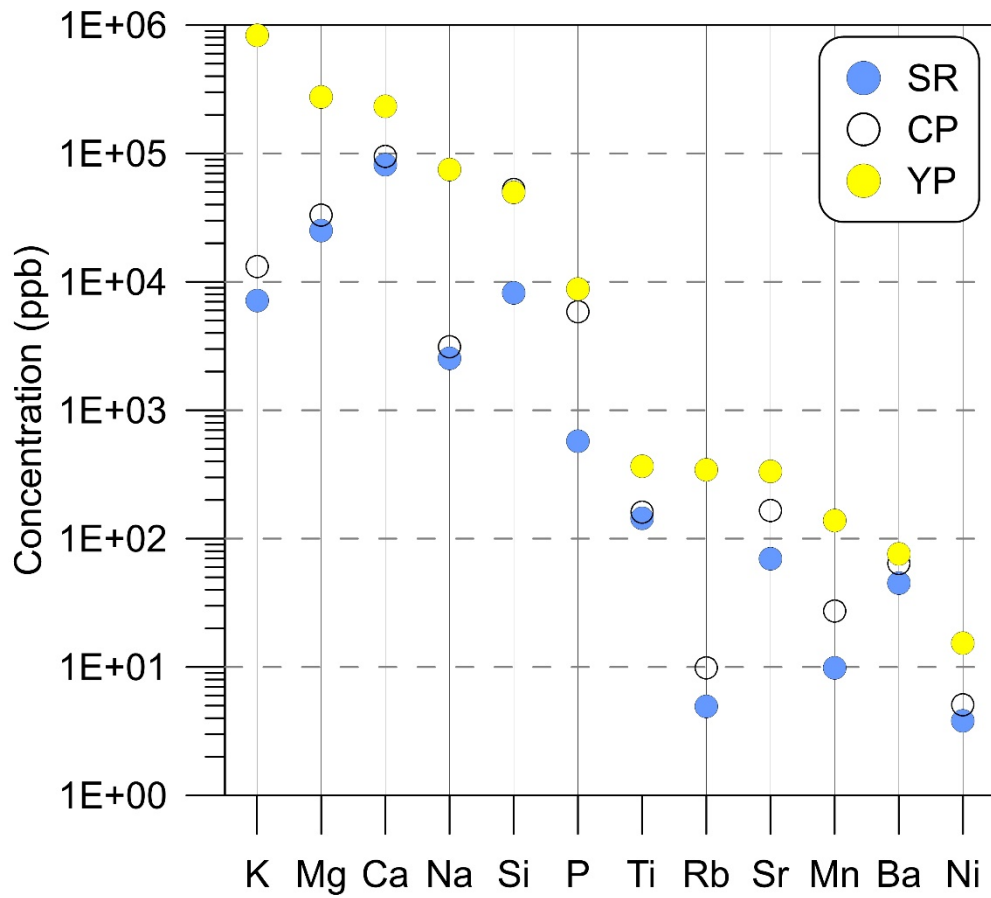
173

174

175 **Figure S3.** Results of U-Th dating of CCCs from Winter Wonderland Cave. The TF sample
 176 formed between 2016 and 2018, so the initial $^{230}\text{Th}/^{232}\text{Th}$ for this sample (6.89×10^{-6}) was used
 177 for all of the samples. 5A and 5C are replicates for sample YS-5. 6A and 6B are replicates for
 178 samples YS-6. Wide error bars are a product of a large correction for detrital ^{230}Th .
 179 Nonetheless, all of the dated samples likely formed during the Holocene, and ages for CP and
 180 YS-6 overlap with modern.

181





187
188

189 **Figure S5.** Abundance of consistently detectable elements in water samples from Winter
190 Wonderland Cave. Sample SR was collected from a pool with a lid of ice in 2019 (Fig. 2b).
191 Samples YP and CP were collected from pools on the ice surface in 2018 (Table S1).
192 Concentration of all solutes is much higher in the YP (Yellow Pool) sample.